Expert Systems with Applications 42 (2015) 7344–7355

Contents lists available at ScienceDirect

Expert Systems with Applications

journal homepage: www.elsevier.com/locate/eswa

Automatic detection of alertness/drowsiness from physiological signals using wavelet-based nonlinear features and machine learning

Lan-lan Chen *, Yu Zhao, Jian Zhang, Jun-zhong Zou

Key Laboratory of Advanced Control and Optimization for Chemical Processes, Ministry of Education, East China University of Science and Technology, Shanghai 200237, PR China

ARTICLE INFO

Article history:
Available online 24 May 2015

Keywords:
Drowsiness detection
Electroencephalogram (EEG)
Eyelid movements
Wavelet decomposition
Nonlinear features
Extreme learning machine (ELM)

ABSTRACT

Physiological signals such as electroencephalogram (EEG) and electrooculography (EOG) recordings are very important non-invasive measures of detecting a person's alertness/drowsiness. Since EEG signals are non-stationary and present evident dynamic characteristics, conventional linear approaches are not highly successful in recognition of drowsy level. Furthermore, previous methods cannot produce satisfying results without considering the basic rhythms underlying the raw signals. To address these drawbacks, we propose a system for drowsiness detection using physiological signals that present four advantages: (1) decomposing EEG signals into wavelet sub-bands to extract more evident information beyond raw signals, (2) extraction and fusion of nonlinear features from EEG sub-bands, (3) fusion the information from EEGs and eyelid movements, (4) employing efficient extremely learning machine for status classification. The experimental results show that the proposed method achieves not only a high detection accuracy but also a very fast computation speed. The proposed algorithm can be further developed into the monitoring and warning systems to prevent the accumulation of mental fatigue and declines of work efficiency in many environments such as vehicular driving, aviation, navigation and medical service.

1. Introduction

Increasing studies have explored the measurements of drowsiness due to its impact on public health, public safety and productivity (Baker et al., 1994; Boksem, Meijman, & Lorist, 2005; Dawson et al., 2014; Folkard & Tucker, 2003). The ability of a person to maintain alert and make decisions quickly decreases considerably during the drowsiness stage (Garcés Correa, Orosco, & Laciar, 2014). Fatigue driving under drowsy even sleepy state is an important determinant of traffic accidents (Azim, Jaffar, & Mirza, 2014; Cyganek & Gruszczyński, 2014; Forsman, Vila, Short, Mott, & Van Dongen, 2013; Hashemi, Saba, & Resalat, 2014; Hu & Zheng, 2009; Jagannath & Balasubramanian, 2014; Jo, Lee, Park, Kim, & Ki, 2014; Li & Chung, 2014). In addition to vehicular safety concern, drowsiness and fatigue are very important issues for workers and employees in the fields of industrial manufactories (Tucker, Folkard, & Macdonald, 2003), power plants (Baker et al., 1994), navigation, aviation (Borghini, Astolfi, Vecchiato, Mattia, & Babiloni, 2014) and medical service.

Physiological measurements such as EEG recordings, eyelid movement, galvanic skin response (GSR), heart rate and pulse rate provide insight into human activities directly and achieve relatively accurate quantification evaluation of drowsiness/alertness (Boksem et al., 2005; Borghini et al., 2014; Dissanayaka et al., 2015; Garcés Correa et al., 2014; Hashemi et al., 2014; Hu & Zheng, 2009; Jagannath & Balasubramanian, 2014; Lal & Craig, 2005; Lee et al., 2014; Li & Chung, 2014; Singh et al., 2013). Among these different measures, EEG is commonly viewed as the "golden standard" in the identification of states ranging from vigilant or alert to drowsy or asleep (Garcés Correa et al., 2014; Johnson et al., 2011).

However, the visual inspection of continuous physiological signals is very arduous and challenging work even for the trained neurologists (Nakamura, Chen, Sugi, Ikeda, & Shibasaki, 2005) since physiological signals are easy to be contaminated by the excessive presence of artifacts and present extensive individual difference. Hence, it is significant to develop the automatic system to liberate the neurologists from long-term EEG interpretation. The goal of this research is to develop an efficient system to detect drowsy/alert epochs which will be applied in: (1) assistance of neurologists to review potential segments of alert and drowsy states for further

* Corresponding author at: Key Laboratory of Advanced Control and Optimization for Chemical Processes, Ministry of Education, East China University of Science and Technology, 130 Meilong Road, Shanghai 200237, PR China. Tel.: +86 21 64253671.
E-mail addresses: chenlanlan104@gmail.com, llchen@ecust.edu.cn (L.-l. Chen), yuzhao.ecust@gmail.com (Y. Zhao), zhangjian@ecust.edu.cn (J. Zhang), jzhzou@ecust.edu.cn (J.-z. Zou).

http://dx.doi.org/10.1016/j.eswa.2015.05.028
0957-4174/

inspection (Nakamura et al., 2005; Shibasaki et al., 2014); (2) monitoring and warning systems for detecting the drowsy states to prevent the accumulation of mental fatigue and declines of work efficiency in real-world operation and living environments (Lin et al., 2008).

Researchers have attempted to develop various algorithms for the automatic detection of drowsiness/alertness based on physiological signals and those studies mainly focus on techniques for feature extraction and classification. Some of the efficient feature extraction methods based on EEG signals are as follows: waveform and statistics from time series (Garcés Correa et al., 2014), power spectral density (Chen et al., 2010; Lal & Craig, 2005), cross spectral density (Vuckovic, Radivojevic, Chen, & Popovic, 2002), wavelet coefficients (Lee et al., 2014; Subasi, 2005), functional coherence (Dissanayaka et al., 2015) and visually evoked potentials (VEP) (Hashemi et al., 2014). Besides, ocular measures, such as eye movement and blink tracking are considered as promising ways for monitoring drowsiness (Hu & Zheng, 2009; Li & Chung, 2014). Some of these studies have been tested on practical systems such as brain-computer interface for monitoring and warning of driver's drowsiness (Azim et al., 2014; Hashemi et al., 2014; Lal et al., 2003; Lin et al. 2008).

Since EEG signals are non-stationary and present evident dynamic characteristics, conventional linear approaches are not highly successful in recognition of drowsy level. Nonlinear methods obtained more popularity in the recent years and the summary of such studies is given in the discussion part of the paper. In this study, we assess and compare four nonlinear methods, i.e., approximate entropy (ApEn), sample entropy (SampEn), renyi entropy (RenEn) and a novel graphic method named recurrence quantification analysis (RQA). Furthermore, recent investigations indicate that some nonlinear measures cannot achieve satisfying performance without considering the basic rhythms of physiological signals (Chen, Zhang, Zou, Zhao, & Wang, 2014). In some cases, EEG separate sub-bands may present more accurate information about constituent neuronal activities underlying EEG signals. The characteristics which are not evident in the original full-spectrum EEG may be distinct in separate sub-bands (Chen et al., 2014). Hence, our proposed system implemented the wavelet decomposition to extract the nonlinear features with different time and frequency scales.

Another important task for the design of an automatic system is to develop a highly sensitive classifier with a low false detection rate. To improve the overall performance of a detection system, the designers must confront a steep tradeoff between detector sensitivity and specificity and make a compromise between detector efficiency and specificity. Some of the reported systems such as driving fatigue detection system (Li & Chung, 2014) was based on the estimation of eye close degree (ECD) using EEG sensors and constructed a support vector machine (SVM) for classification. Garcés Correa et al. (2014) developed an automatic method to detect the drowsy status in EEG records based on time, spectral and wavelet analysis and the selected features were fed to a neural network classifier. Artificial neural network (ANN) (Garcés Correa et al., 2014; Singh et al., 2013; Subasi, 2005; Vuckovic et al., 2002) and support vector machine (SVM) (Hu & Zheng, 2009; Jo et al., 2014; Lal & Craig, 2005; Lee et al., 2014; Yeo et al., 2009; Zhao, Zheng, Zhao, Tu, & Liu, 2011) have been widely explored as the detector for classification. However, when the sample size is large, the learning speed of both methods is too slow to meet the requirements for real-time applications. SVM may perhaps tend to achieve suboptimality in classification applications due to some optimization constraints. A novel learning algorithm named extreme learning machine (ELM) (Huang, Zhu, & Siew, 2006) can not only avoid falling into local optima but also largely improve the learning speed. In this research, the wavelet-based nonlinear features were fed to the ELM classifier for detecting drowsy/alert states with overall consideration of detector sensitivity, specificity and efficiency.

2. Materials

2.1. Participants and experiment task

Sixteen healthy male students participated in this experiment, ranging in age from 22 to 25 years old. Subjects were required to keep a sleep diary one week prior to the experiment to ensure that they had at least 7 h of continuous sleeping time and regular sleeping hours. Thirteen subjects who reported good and regular sleep were finally selected for this study. Subjects were instructed to abstain from prescription medication, alcohol and caffeine 24 h before experiments. The experiments were performed according to the Declaration of Helsinki. The project protocol was approved by the local Institutional Review Board (IRB) of East China University of Science and Technology. The subjects gave their informed consent prior to the experiments.

The experiment task started around 3:00 p.m., which corresponded to the afternoon sleepiness peak in the human circadian rhythm (De Gennaro et al., 2001; Yeo et al., 2009). Subjects performed mental calculation for continuous two hours in which the subject's attempts at maintaining vigilance were dependent on their own determination to stay awake. During the experiment subjects were settled in a separate cubicle and no feedback of calculation performance was presented to the subjects, thereby reducing external disturbances and providing an environment conducive to sleep.

2.2. Data acquisition

Night-channel EEG signals were recorded by a digital EEG machine (Nihon-Koden EEG 2110) with the sampling frequency of 256 Hz. Electrodes were positioned at Fp1, Fp2, F3, F4, Fz, Cz, O1, O2 and Oz against ipsilateral earlobe electrode (A1, A2 or the average of A1 and A2) according to the standard 10–20 system. Additionally, two-channel EOG signals were recorded to analyze blink activities as part of the classification criteria for both visual inspection and automatic detection.

2.3. Data preparation

The artifact was removed from the recording by visual inspection. Two neurologists manually selected the segments used in this study. Each of them inspected the EEG/EOG recordings according a detailed criterion using three identifiers: (1) eye blink patterns (2) dominant EEG activity (3) frontal midline theta rhythm.

The 'alert' state refers to relaxed wakefulness with the presence of dominant beta rhythm (13–25 Hz) (Yeo et al., 2009) and quick blink activities (Doughty, 2002). The 'drowsy' state is recognized when EEG showing the presence of slow eye movement with occipital alpha rhythm (9–13 Hz), a decrease in the amplitude and/or frequency of the alpha rhythm (alpha dropout) (Yeo et al., 2009). The frontal midline (Fm) theta rhythm appears when some healthy subjects are under light drowsiness engaged in a mental task (Takahashi, Shinomiya, Mori, & Tachibana, 1997). Fm theta is induced not only during mental tasks but also during sleep stages and it appears during rapid eye movement (REM) and stage 1 of non-REM (NREM) sleep (Inanaga, 1998). Individual difference should be taken into account during the usage of dominant rhythm and Fm theta. Each of the neurologists inspected the EEG recordings using the above criteria and then agreed which EEG sequences clearly indicated a drowsy or alert state. The segments with

ambiguities events were excluded from the analysis. The manually classified EEG segments agreed by both neurologists were further analyzed. Finally, 100 drowsy segments and 126 alert segments were selected and each segment contained 2048 samples (8 s). To simulate the identification process of neurologists, two efficient EEG channels, i.e., Fz and Oz additionally with two EOG channels were used for the further analysis of the automatic system.

3. Methods

3.1. System overview

The flow chart for the detection procedure is shown in Fig. 1. First, two neurologists interpret the acquired EEG/EOG signals and mark the recordings used for this study. Then, the selected EEG segments are decomposed into sub-band signals by wavelet transform. Four nonlinear features, i.e., approximate entropy (ApEn), sample entropy (SampEn), renyi entropy (RenEn) and recurrence quantification analysis (RQA) are computed and fused then fed to classifiers. For the purpose of comparison with the wavelet-based nonlinear methods, the conventional FFT-based spectral features are also computed and fed to the same classifiers. To improve the detection performance, complementary features extracted from blink activities are combined with EEG features as the input information for classifiers.

In this study, an efficient classifier – extreme learning machine (ELM) is utilized to determine the class membership of these feature vectors: 1 – drowsiness, 0 – alertness. Two kinds of ELM, i.e., basic ELM with sigmoid activation function (non-kernel case) and ELM with RBF network (kernel case) are tested. The performance of ELM is compared with another detector – support vector machine (SVM) in terms of accuracy and consuming time.

3.2. Wavelet decomposition

Since the sampling frequency of the EEG is 256 Hz, the maximum available frequency is half of the sampling frequency, i.e., 128 Hz. A five-level wavelet decomposition is utilized to EEG data and the frequency bands of decomposed signals are shown in Fig. 2. The decomposed components, e.g., a5, d5, d4, d3 and d2, approximately correspond to the basic physiological EEG rhythms, i.e., delta (0.5–4 Hz), theta (4–8 Hz), alpha (8–13 Hz), beta (13–30 Hz) and gamma (30–60 Hz). Considering the correlation between the analyzing signal and the mother wavelet, Daubeehies 4 (db4) wavelet family is used.

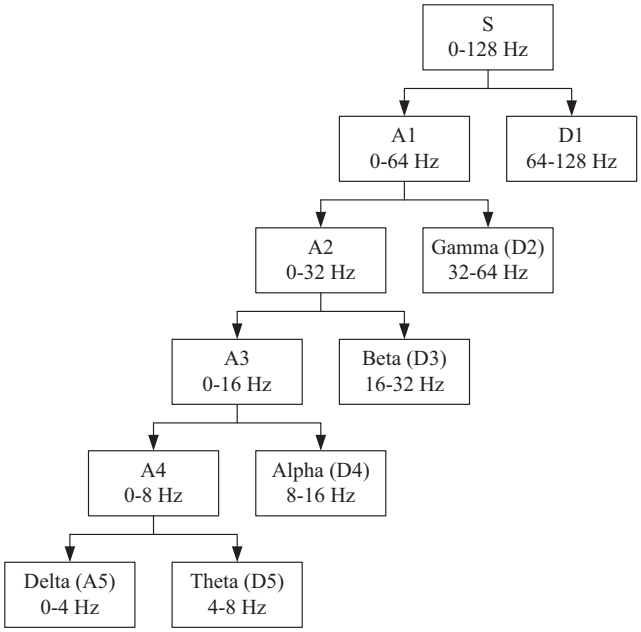

Fig. 2. Wavelet decomposed signal and corresponding frequency band.

3.3. Approximate entropy

Approximate entropy (ApEn) is used to quantify the complexity or irregularity of a signal and describes the rate of producing new information. A high value of ApEn reflects random and unpredictable variation, whereas a low value of ApEn indicates regularity and predictability in a time series (Burioka et al., 2005). As introduced by Pincus (1991), ApEn is derived from the correlation integral $\Phi_i^m(r)$, which measures the frequency of patterns similar to the one given by the embedding dimension m within a tolerance window r.

The ApEn is computed as:

$$\mathrm{ApEn}(m,r,N) = \Phi^m(r) - \Phi^{m+1}(r). \tag{1}$$

$$\Phi^m(r) = \frac{1}{N-m+1}\sum_{i=1}^{N-m+1} \ln \Phi_i^m(r). \tag{2}$$

More details about ApEn algorithm can be found in Pincus (1991). The setting of parameters should insure a high discrimination rate

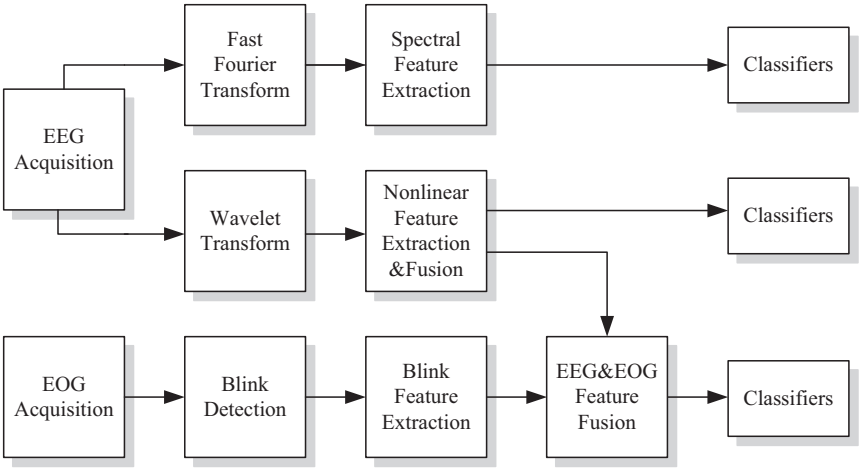

Fig. 1. Flow chart for the complete procedure.

between drowsy and alert states. Usually, m is set to be 1, 2 or 3 and r is set to be some percentage of the standard deviation of the amplitude of time series. In this research, m is set to be 2 and r is set to 20% percentage. N is set to 2048.

3.4. Sample entropy

The ApEn counts each sequence as matching itself to avoid the occurrence of ln(0) in the process of calculation, which will lead to the bias of ApEn (Al-Angari & Sahakian, 2007). In practice, this bias causes two important drawbacks of ApEn. First, ApEn is heavily dependent on the length of record; Second, it lacks relatively consistency. To reduce this bias, Richman and Moorman (2000) proposed a new method named sample entropy (SampEn) which had two differences from ApEn. First, SampEn does not count self-matches. Second, SampEn does not use a template-wise approach when estimating conditional probabilities. Mathematically, the computation of SampEn has the similar steps to ApEn. Note that the self matched templates are not computed. Then

$$\mathrm{SampEn}(m,r,N) = \ln\left[\Phi^m(r) - \Phi^{m+1}(r)\right]. \tag{3}$$

$$\Phi^m(r) = \frac{1}{N-m+1}\sum_{i=1}^{N-m+1}\Phi_i^m(r). \tag{4}$$

More details about the computing process of SampEn are introduced in Richman and Moorman (2000). In this research, m, r and N have the same settings as those of ApEn.

3.5. Renyi entropy

Renyi entropy (RenEn) can be conceptualized as superclass of Shannon entropy (ShanEn) (Cornforth, Tarvainen, & Jelinek, 2013; Renyi, 1960) and is given by

$$I_\alpha = \frac{1}{1-\alpha}\log\left(\sum_{i=1}^{n} p_i^\alpha\right) \tag{5}$$

where p_i is the probability of occurrence of an event (feature value) x_i being an element of the event (feature) X that can take values $\{x_1 \ldots x_n\}$. When α approaches 1, RenEn converges to ShanEn. RenEn has similar properties as the ShanEn: it is additive and it has maximum = $\ln(n)$ for $p_i = 1/n$. But it contains additional parameter α which can be used to make it more or less sensitive to the shape of probability distributions.

3.6. Recurrence quantification analysis

Eckmann, Kamphorst, and Ruelle (1987) presented a graphic method called recurrence plot (RP) to detect patterns of recurrence in the data which was one of the most important characteristics of dynamic systems. However, being a tool of a visual and qualitative nature, its results were not always conclusive. To overcome this drawback, Webber and Zbilut (1994) developed it by quantifying differently appearing recurrence plots (RPs) based on the small-scale structures and named the developed method "recurrence quantification analysis" (RQA). In the recent past, RQA has been successfully applied to analyze noisy and non-stationary data. More details of recurrence plot analysis can be found in Webber and Zbilut (1994), Zbilut, Thomasson, and Webber (2002) and Marwan, Romano, Thiel, and Kurths (2007).

Fig. 3 illustrates the EEG time series and their corresponding recurrence plots (RPs) at drowsy and alert status. The drowsy state presents the occipital alpha rhythm (Fig. 3a upper) and the alert state shows dominant beta rhythm (Fig. 3b upper). Their RPs display different structures. In order to go beyond the visual impression yielded by RPs, several recurrence quantification estimators are assessed in this paper, i.e., %REC, %DET, ENTR, LAM, TT, V_{max}, L_{max}, T1 and T2. The parameters selection should insure that %REC < 1 (Webber & Zbilut, 1994; Zbilut et al., 2002). The embedding dimension can be determined by using the mutual information method and the false nearest neighbor method. The general computing process of RQA estimators is given in Appendix A.

3.7. Frequency spectral analysis

For the purpose of comparison with the wavelet-based nonlinear methods, the conventional FFT-based spectral features are computed. Power Percentage (PP) is analyzed using EEG spectrum power in each frequency band divided by those in the total spectrum range.

Additionally, two frequency estimators are computed.

Gravity frequency (GF): It is defined as

$$GF = \frac{\sum_i P(f_i)\times f_i}{\sum_i P(f_i)} \tag{6}$$

where f is frequency and $P(f_i)$ is the estimated power spectral density.

Frequency variability (FV): It is defined as

$$FV = \frac{\sum_i P(f_i)\times f_i^2 - \frac{\left(\sum_i P(f_i)\times f_i\right)^2}{\sum_i P(f_i)}}{\sum_i P(f_i)} \tag{7}$$

This feature describes the variance of the frequency in the defined frequency band.

3.8. Blink activities and features

The first task for EOG signal analysis is to identify blink activities. Using the algorithm introduced by Hu and Zheng (2009), approximately 95% of the blink events are correctly identified. Three basic parameters are extracted from the detected blinks, i.e., the number of blinks (NB), the duration of blink (DB) and the intervals between blinks (IB). The detailed description is given in Table 1.

3.9. Classifiers

Huang, Zhu, and Siew (2006) proposed a novel learning algorithm called extreme learning machine (ELM) based on the single-hidden layer feed-forward neural networks (SLFN). Usually, it is very time consuming for almost all practical feed-forward neural networks. While ELM randomly chooses the input weights and hidden layer biases only with the output weights analytically determined, it can easily achieve good generalization performance with extremely fast learning speed. Huang (2014) extends ELM to SLFNs with radial basis function (RBF) kernels which randomly generate the centers and impact widths of RBF kernels and simply analyze the output weights instead of iteratively tuned. In this experiment, two kinds of ELM, i.e., basic ELM with sigmoid activation function and ELM with RBF kernels are tested. The ELM can achieve the best classification results with 20 hidden neurons and there is one node in the output layer whose target value is defined as: 1 – drowsiness, 0 – alertness. The general process of ELM algorithm is explained in Appendix B and the difference between kernel and non-kernel cases is discussed in detailed in Huang (2014).

For the purpose of comparison with ELM, support vector machine (SVM) is also applied. For the SVM classifier, RBF kernel

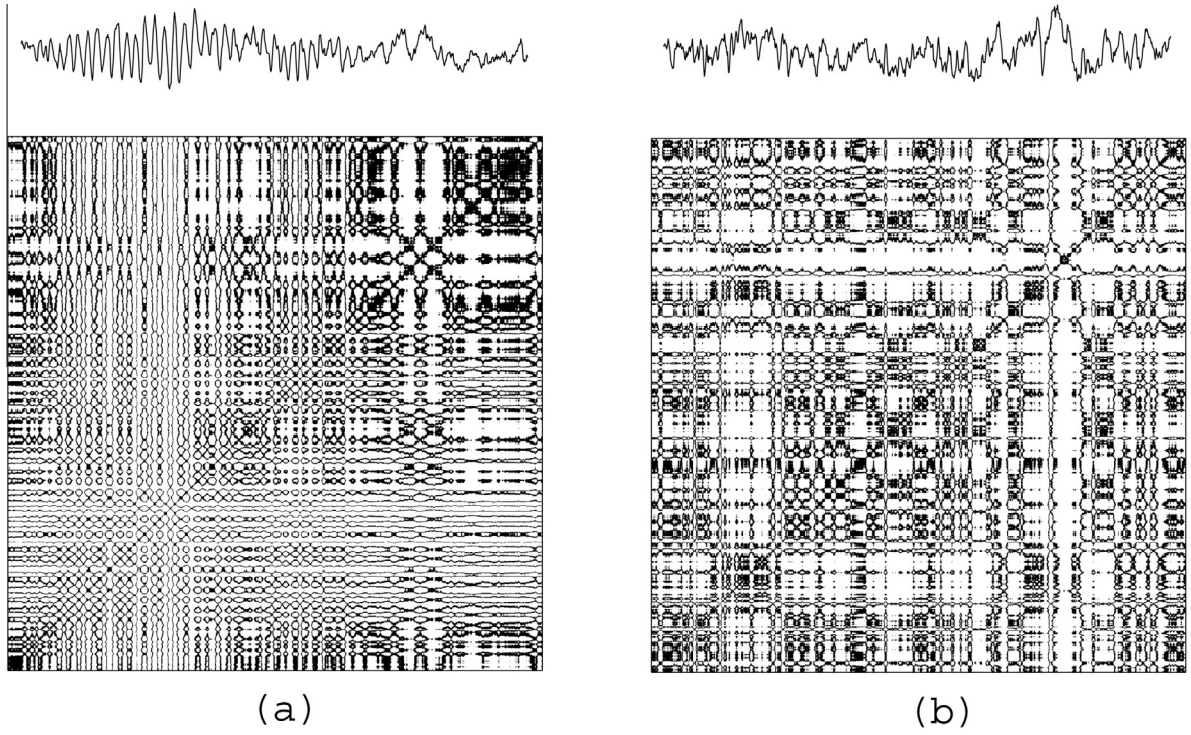

Fig. 3. Recurrence plots (RPs) of EEGs. (a) EEG segment at drowsy state and its RP and (b) EEG segment at alert state and its RP.

Table 1
The blink features.

Variables	Description	Comment
NB	The number of blinks	The number of blink events detected in each segment
DB	Duration of blink	Calculated from the start position of blink to the end value of blink
IB	Interval between blinks	Calculated the intervals between the peak position of two adjacent blinks

is chosen as kernel function and for model selection ten-fold cross-validation on training data is used.

4. Results

4.1. Characteristics based on wavelet nonlinear analysis

Four nonlinear methods were applied to the explained dataset. First, original EEG signals and their corresponding sub-bands were analyzed separately. Then combination of features extracted from these sub-bands was analyzed.

Fig. 4 illustrates the ApEn of drowsy and alert EEG epochs. The *y*-axis represents the value of ApEn. From Fig. 4a, we can see considerable overlap of drowsy and alert states computed from the original full-spectrum EEG signals. After the wavelet decomposition, the difference between the two distinct states became more clearly especially in the d3, d4, d5 and a5 sub-band signals (Fig. 4d–g). Further, combined features from sub-bands showed the best discrimination (Fig. 4h). Besides, SampEn, RenEn and RQA features presented the similar phenomenon.

Fig. 5 presents the receiver operating characteristic (ROC) curves in which the characteristics of raw signals and the union of sub-band signals are compared. Usually, ROC curve is used as a graphical tool to represent the relationship between true positive rate (TPR, also named sensitivity) and false positive rate (FPR, FPR = 1 − specificity) as a threshold parameter is varied. The area under the ROC curve (ROC–AUC) is an effective measure to compare the performance of different features or classifiers (Zweig & Campbell, 1993). From Fig. 5, it was observed that the combination of wavelet sub-bands yielded in larger areas than those of the raw signals not only for the four separate nonlinear methods but also for the fusion of these four methods. Particularly, the ROC–AUCs of ApEn and SampEn computed from the orignal signals were slightly larger than 0.5 which were close to the results from random discrimination but the performance for the combination of sub-bands improved significantly.

4.2. Comparison of detection performance

A leave-one-out cross validation method was used in the proposed detection system. All but one subjects' data was trained for the classifier. The withheld subject's data was used for testing. This process was repeated *N* times (*N* was the amount of subjects) so that each subject's data has been tested.

The performance of the three classifiers, i.e., the basic ELM, ELM with RBF kernels and SVM classifiers, can be assessed by the measures of sensitivity, specificity, recognition accuracy and consuming time.

- Sensitivity (Sens.): number of true positives/the total number of drowsy samples labeled by the neurologists. True positive represents the drowsy EEG segment identified by both the computer programs and the neurologists.
- Specificity (Spec.): number of true negatives/the total number of alert samples labeled by the neurologists. True negative indicates the alert EEG segment recognized by both the computer programs and the neurologists.
- Recognition accuracy (Acc.): number of correctly identified samples/total number of samples.
- Consuming time: the machine time consumed on both training and testing processes.

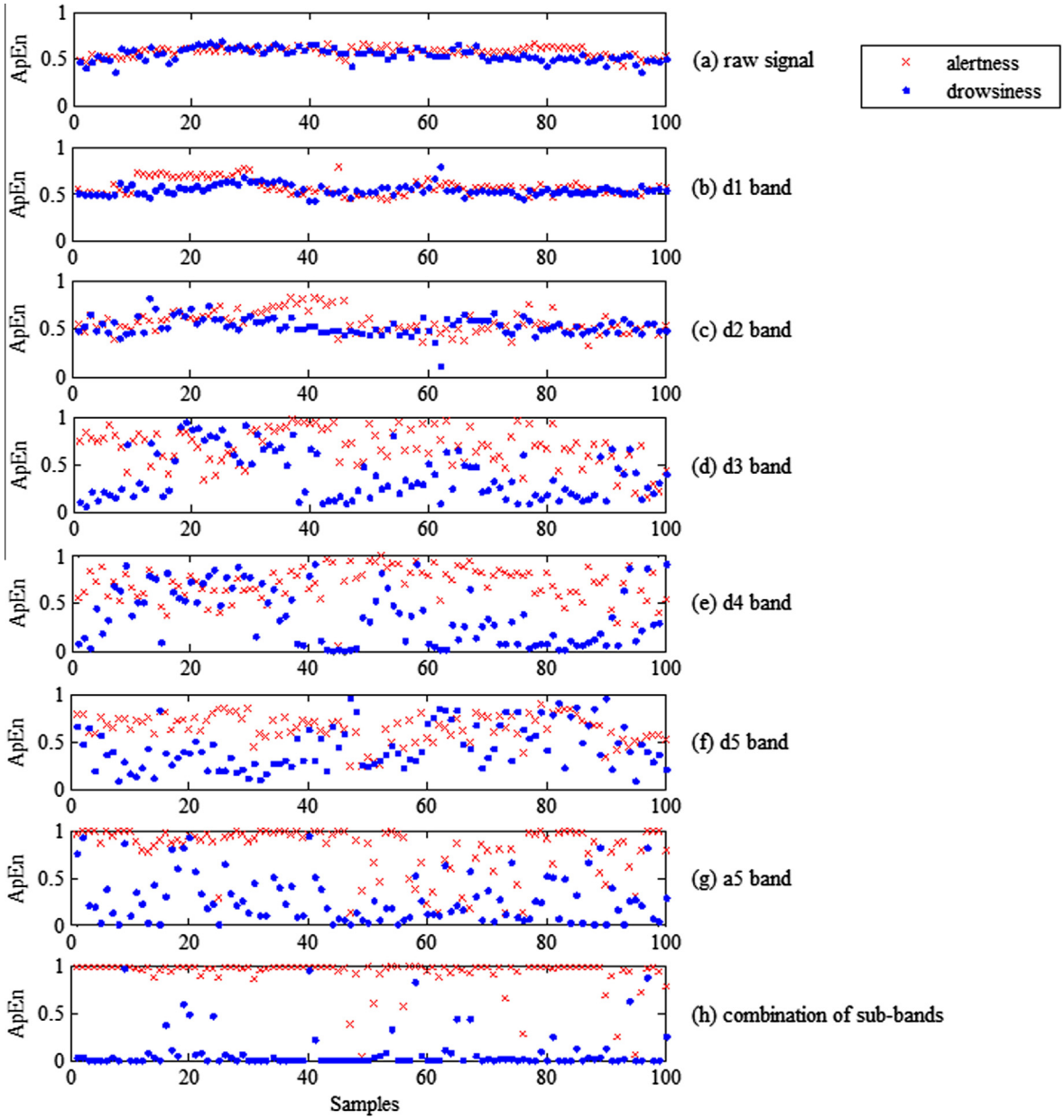

Fig. 4. The comparison of ApEn between drowsy and alert EEG. (a) Features computed from the original full-spectrum EEG signals. (b)–(g) Features computed from the sub-band signals {d1, d2, d3, d4, d5, a5} respectively. (h) Combination of the sub-band features.

First, the true detections and false detections were computed for each subject under the leave-one-out cross-validation tests. Then the overall performance was analyzed based on the total number of true/false detections for all subjects. The consuming time was an averaged value of machine time spent on each subject. The detection performance using four wavelet nonlinear features and conventional FFT measures were listed in Table 2 with the sequence of the recognition accuracy from low to high values. It was observed that all the four wavelet-based nonlinear features achieved higher recognition accuracy than that of the classic FFT-based spectral measures. Furthermore, fusion of four wavelet nonlinear methods presented the best discrimination performance.

Additionally, the experimental results show that the ELM can complete learning at extremely fast speed and produce comparable discrimination performance to that of SVM. In the cases of wavelet SampEn, wavelet RQA and fusion of nonlinear features, ELM algorithm with RBF networks showed stronger discriminatory power than that of SVM.

Furthermore, Table 3 presents the improvement of recognition accuracy after fusion with EOG information. After combining with EOG measures, the fusion of EEG nonlinear features using ELM_RBF detector achieved the best recognition accuracy of 97.3%.

5. Discussions

5.1. Review of the similar work

Research has shown that sustained attention or vigilance declines over time on task. Sustained attention is necessary in many environments such as driving conditions, navigation, aviation, medical service and securities transaction. A lapse of attention in any one of these environments will cause human casualties or/and property losses. Commonly, there are three ways to monitor the vigilance level: the methods based on behavior performance (Folkard & Tucker, 2003; Forsman et al., 2013); the technique based on visual features (Jiménez-Pinto & Torres-Torriti, 2013;

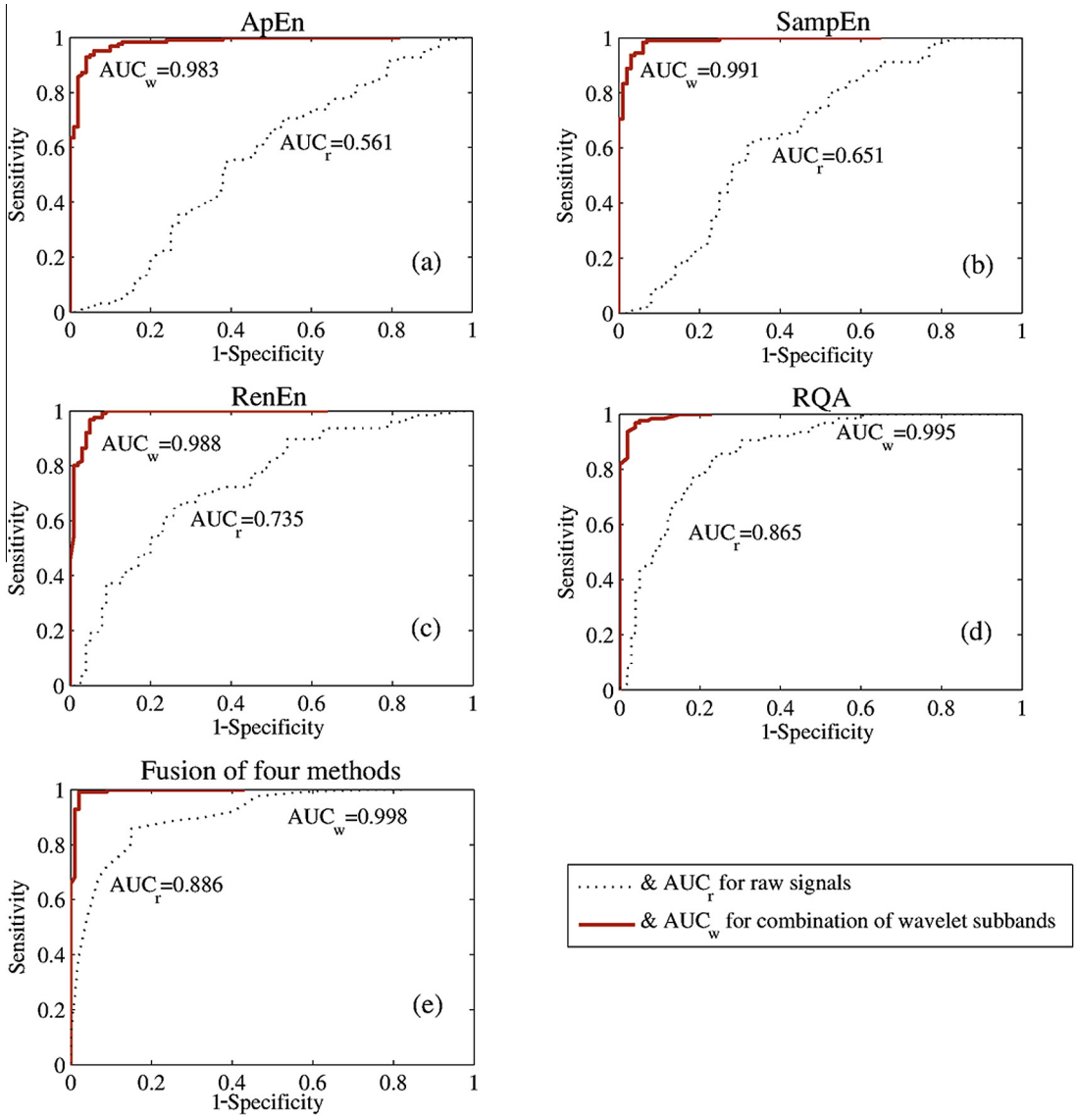

Fig. 5. ROC curves and ROC–AUCs (the area under ROC curve) for four nonlinear features and the fusion of these features. Dashed curves and AUC_r are computed from the raw full-spectrum signals; Solid curves and AUC_w are computed from the combination of wavelet sub-band signals.

Wu and Chen; Azim et al., 2014; Cyganek & Gruszczyński, 2014; Jo, Lee, Park, Kim, & Ki, 2014; McIntire, McKinley, Goodyear, & McIntire, 2014) and the analysis based on physiological signals (Borghini et al., 2014; Dissanayaka et al., 2015; Garcés Correa et al., 2014; Hashemi et al., 2014; Jagannath & Balasubramanian, 2014; Lee et al., 2014; Li & Chung, 2014; Singh et al., 2013).

Methods based on behavior performance, for example in the driving conditions, usually assess the estimators such as vehicle speed, acceleration, steering, braking and gear changes (Dawson et al., 2014; Forsman et al., 2013). The main drawback of these methods is that the individual difference of the vehicle and its driver always exist.

Currently, drowsiness detectors using video based technology that track facial and/or head movements and eye gaze monitoring are being widely studied (Azim et al., 2014; Cyganek & Gruszczyński, 2014; Jiménez-Pinto & Torres-Torriti, 2013; Jo et al., 2014; McIntire et al., 2014; Wu & Chen, 2008). Jo et al. (2014) proposed a driver drowsiness detection method by fusing information from both eyes providing robust performance under a variety of conditions. Azim et al. (2014) monitored the information of eyes and mouth and further passed them to fuzzy expert system (FES) yielding an average accuracy of 100%. However, some drawbacks such as brightness limitations, glass wearing problem and practical hurdles such as distraction of the drivers should be taken into account. Cyganek and Gruszczyński (2014) presents a vision system for driver's eye recognition, which consists of two cameras operating in the visual and near infra-red (NIR) spectra allowing the operation both in day and night conditions. However, when drivers observed longer exposures to NIR they can be tiresome even dangerous. Besides, the system will be limited when drivers are wearing dark sunglasses.

Recently, the methods based on signal processing techniques that utilize information from physiological signals such as electroencephalography (EEG), electrocardiography (ECG), electrooculography (EOG) and electromyography (EMG) recordings show good detection accuracy and provide insight into the nature of fatigue. A great number of "physiological signals based method" for drowsiness detection have been studied (Borghini et al., 2014; Dissanayaka et al., 2015; Garcés Correa et al., 2014; Hashemi et al., 2014; Jagannath & Balasubramanian, 2014; Lee et al., 2014;

Table 2
Results using wavelet-based nonlinear features versus those of conventional FFT methods.

Features	Classifiers	Performance			
		Sens. (%)	Spec. (%)	Acc. (%)	Time (s)
FFT	ELM_sig	88.1	75.0	82.3	0.112
	ELM_RBF	87.3	74.0	81.4	0.112
	SVM	87.3	76.0	82.3	26.386
Wavelet_ApEn	ELM_sig	89.7	87.0	88.5	0.110
	ELM_RBF	92.1	84.0	88.5	0.109
	SVM	90.5	86.0	88.5	26.029
Wavelet_RenEn	ELM_sig	89.7	90.0	89.8	0.101
	ELM_RBF	88.9	90.0	89.4	0.098
	SVM	89.7	90.0	89.8	24.640
Wavelet_SampEn	ELM_sig	93.7	89.0	91.6	0.109
	ELM_RBF	95.2	88.0	92.0	0.111
	SVM	92.1	87.0	89.8	25.686
Wavelet_RQA	ELM_sig	92.9	90.0	91.6	0.134
	ELM_RBF	96.0	92.0	94.3	0.135
	SVM	95.2	88.0	92.0	34.926
Fusion of four wavelet nonlinear features	ELM_sig	96.0	93.0	94.7	0.165
	ELM_RBF	***96.8***	***94.0***	***95.6***	0.166
	SVM	96.0	93.0	94.7	42.010

The best performance of sensitivity, specificity and accuracy has been marked in bold, italics and underline.

Li & Chung, 2014; Singh et al., 2013). Li and Chung (2014) presented a novel way to compute the eye closure degree (ECD) using EEG sensors instead of video-based methods, which not only addressed the video-based method drawbacks, but also made ECD estimation more computationally efficient and easier to implement in EEG sensors in a real time way. Garcés Correa et al. (2014) developed an algorithm using a multi-modal analysis of the EEG and artificial neural networks (ANN) to detect the drowsiness stage yielding more than 80% of detection accuracy. A limitation of Garcés Correa's work is that the results of the proposed detector have been obtained processing EEG records from polysomnographic studies. Borghini et al. (2014) observed a coherent sequence of changes from EEG, EOG and other physiological signals occurred during the transition from normal, light drowsiness and eventually mental fatigue. Jagannath and Balasubramanian (2014) evaluated the early onset of driver fatigue during simulated driving test from multiple physiological signals such as surface electromyography (sEMG), electroencephalography (EEG), heart rate and etc.

The results gathered by the vigilance tasks using vehicular driving simulators (Jagannath & Balasubramanian, 2014) and air force-relevant simulators (McIntire et al., 2014) could reflect the disadvantage of not being generalized to real-life environments because some subjects in driving and controlling simulators are alert because it is an interesting test for them and the drowsiness episodes are not as spontaneous as in real life. In our study, subjects were settled in a quiet cubicle to do mental work as in daily life in which the subjects' attempts at maintaining vigilance were dependent on their own desire and no feedback of behavior performance were presented to the subjects, thereby reducing external disturbances and providing an environment conducive to spontaneous drowsiness. Therefore, the outcome of our study could be extended to real life environments to detect the attention level since all the features were extracted from real and spontaneous physiological recordings.

The system developed by Hashemi et al. (2014) was based on the information of Visually Evoked Potentials (VEP) and approached an accuracy of 97% for the detection of driver's sleepiness. Since the Steady State VEPs (SSVEPs) are responses of human brain to the external visual stimuli such as flickering LED, it is easy to cause the distraction and visual fatigue of drivers.

In this research, we developed a system to detect the drowsiness during sustained mental work based on the analysis of spontaneous EEG recordings and eyelid movements. Since physiological signals are non-stationary and present evident dynamic characteristics, it is generally argued that nonlinear measures are likely to give more information than the ones obtained with conventional approaches such as waveform statistics (Garcés Correa et al., 2014), power spectral density (Chen et al., 2010; Lal & Craig, 2005), wavelet coefficients (Lee et al., 2014; Subasi, 2005) and functional coherence (Dissanayaka et al., 2015). The following sections discuss the effectiveness of wavelet nonlinear methods and efficiency of the detector proposed in our system.

5.2. The merits of wavelet based nonlinear methods

The ability to reflect nonlinear characteristics of the signal makes entropy estimator a well-qualified candidate for characterization of nonlinear dynamics. The advantage of entropy estimator is that it is very effective for the analysis of short-length time series and resistant to short transient data. In the literature, fatigue, sleepiness and drowsiness, are often used synonymously. For instance, approximate entropy (ApEn) has already been applied into the estimation of different sleep stages (Burioka et al., 2005) and mental fatigue levels (Liu, Zhang, & Zheng, 2010). Zhang and Chen (2012) reported a significant decrease of sample entropy (SampEn) under drowsy state compared with those under conscious state. Bruce, Bruce, and Vennelaganti (2009) reported SampEn could track the changes in EEG power spectrum with sleep state and aging. Furthermore, recurrence quantification analysis (RQA) can measure the complexity of non-stationary and noisy data when other methods fail. Gao, Cao, Gu, Harris, and Principe (2003) used recurrence time statistics to detect the weak transitions in signal dynamics. Song, Lee, and Kim (2004) suggested the information obtained from RQA of sleep EEGs was valuable for analyzing sleep stages in subjects with sleep apnea syndrome.

However, our experimental results demonstrate some of the nonlinear methods cannot obtain good performance without considering the basic rhythms of EEG signals. Since EEG signals are non-stationary, the conventional method using time series analysis or frequency analysis is not highly successful in recognition of drowsiness level. Recent literature reported the application using wavelet transform in the analysis of EEG signals for drowsiness detection; however only basic wavelet coefficient was extracted

Table 3
Improvement of recognition accuracy after fusion with EOG information.

Classifiers	%	EEG features used for combining with EOG measures									
		ApEn		RenEn		SampEn		RQA		Fusion of four nonlinear methods	
		EEG	EEG + EOG	EEG	EEG + EOG	EEG	EEG + EOG	EEG	EEG + EOG	EEG	EEG + EOG
ELM_sig	Acc.	88.5	91.6	89.8	92.9	91.6	93.4	91.6	94.3	94.7	96.9
ELM_RBF	Acc.	88.5	93.4	89.4	93.8	92.0	94.7	94.3	96.5	95.6	97.3
SVM	Acc.	88.5	89.8	89.8	94.3	89.8	94.7	92.0	94.7	94.7	96.9

as features (Lee et al., 2014; Subasi, 2005). In this research, wavelet decomposition makes nonlinear features able to gain much better discriminatory power. Wavelet decomposition extracts the data characteristics with different resolutions and presents more evident information in some sub-band signals than that in original full-spectrum EEG signals (Fig. 4a–g). Further, the combination of useful information helps to improve the accuracy of identification (Fig. 4h). With the help of wavelet decomposition, nonlinear methods present superior performance to that of the same classifiers trained on the classic spectrum features (Table 2).

5.3. The effectiveness of proposed ELM detector

Mainly, artificial neural network (ANN) (Garcés Correa et al., 2014; Singh et al., 2013; Subasi, 2005; Vuckovic et al., 2002) and support vector machine (SVM) (Hu & Zheng, 2009; Jo et al., 2014; Lal & Craig, 2005; Lee et al., 2014; Yeo et al., 2009; Zhao, Zheng, Zhao, Tu, & Liu, 2011) have been widely applied as the detectors in the drowsiness detection system. However, the learning speed of both methods is too slow to meet the requirements in real-world operation and living environments since it will meet a large amount of data during the long time recording. In this research, the proposed extremely learning machine (ELM) can complete learning phase at very fast speed and provide more compact network, which makes it feasible in the application of automatic detection system. The main reason why the learning efficiency of ELM is better than that of the conventional gradient-based learning algorithms lies in: the ELM randomly chooses the input weights and hidden layer biases and analytically determines the output weights without complex iterative operations (Huang et al., 2006). In the kernel case, the ELM arbitrarily assigns the kernels instead of tuning them (Huang, 2014). Compared with the popular SVM, the proposed ELM can be used easily and provide comparable even better discrimination accuracy.

6. Conclusions

This research proposed a framework based on wavelet nonlinear features and machine learning for the automatic identification of drowsiness/alertness that can be applied into the intelligent monitoring and warning systems to prevent mental fatigue, accidents and declines of work efficiency in real environments such as air traffic controllers, cyber operators, and imagery analysts. The proposed method has four advantages in comparison with the previous methods. First, wavelet decomposition helps to extract more evident characteristics underlying the raw signals. Second, the application of nonlinear theory enables us to estimate the nonlinear properties and complexity of physiological signals providing more accurate information than the conventional linear approaches. Third, feature-level fusion method improves the overall detection performance. Finally, the proposed detector using extremely learning machine (ELM) not only produced comparable detection accuracy with the popular SVM but also achieved a very fast learning speed since the factor of computation speed is very important for practical application in expert and intelligent systems.

The limitation of this work can be summarized as follows. First, although physiological features achieve good detection performance, they also depend on peripheral measuring equipment that must be attached to the driver's body. In some sense, it may make body cumbersome and cause activity limitation. Second, nonlinear measures can be viewed as well-qualified candidates for characterization of brain dynamics but these estimators highly depend on the setting of estimation parameters such as embedding dimension and time delay of phase space reconstruction. The selection of estimation parameters needs prior knowledge and experience. Third, this research only designed single task, i.e., sustained mental calculation to induce the spontaneous drowsiness. Since sustained attention is necessary in many environments, more kinds of working scenes and tasks should be considered.

In future, several suggestions should be taken into account. First, use less electrodes and wireless acquisition technique to make the subjects feel more comfortable and freer during the recording process. Second, improve the computation efficiency and robustness of nonlinear measures. Third, test the automatic detection algorithm in more work scenes such as visual target tracking task, simulated and real driving conditions.

Acknowledgement

This work is partly supported by National Natural Science Foundation of China (Nos. 61201124, 51407078) and Fundamental Research Funds for the Central Universities (WH1414022, WJ1313004-1). We acknowledge the assistance of Takenao Sugi at Saga University in experiment design and Masatoshi Nakamura for meaningful discussions and helpful comments.

Appendix A. Recurrence quantification analysis

The parameters of recurrence quantification analysis (RQA) are extracted from the recurrence plots (RPs). An RP can be mathematically defined as:

$$R_{i,j} = \begin{cases} 1, & \text{if } \|X_i - X_j\| < \varepsilon \\ 0, & \text{if } \|X_i - X_j\| \geqslant \varepsilon \end{cases} \tag{A-1}$$

where $\|\cdot\|$ can be Euclidean, maximum and minimum distances. $\{X_i,\ i = 1, 2, \cdots, N\}$ represents certain trajectory of a given scalar time series in a m-dimensional space with a delay time τ. ε means a radius or a threshold. Several estimators are defined as follows:

(1) Recurrence Rate (%REC), which is the density of recurrence dots in a recurrence plot. It is calculated by

$$\%\text{REC} = \frac{1}{N^2}\sum_{i,j=1}^{N} R(i,j) \tag{A-2}$$

(2) Determinism (%DET), which is the ratio of recurrence dots on the diagonal structures to all recurrence dots. It is calculated by

$$\%\text{DET} = \sum_{l=l_{\min}}^{N} lP(l) \Big/ \sum_{i,j}^{N} R_{i,j} \tag{A-3}$$

where $P(l)$ is the frequency distribution of the lengths of the diagonal structures in the RP. $l_{\min}$ is the length of the minimal diagonal line.

(3) Entropy (ENTR), which refers to the Shannon Entropy of the frequency distribution of the diagonal line lengths. It is calculated by

$$\begin{aligned} &\text{ENTR} = -\sum_{l=l_{\min}}^{N} p(l)\ln p(l), \\ &\text{where } p(l) = P(l)/\sum_{l=l_{\min}}^{N} P(l) \end{aligned} \tag{A-4}$$

(4) Laminarity (LAM), which is the fraction of recurrence points that form vertical lines and corresponds to the amount of laminar states in the system. It is given by

$$\mathrm{LAM} = \frac{\sum_{v=v_{\min}}^{N} vP(v)}{\sum_{v=1}^{N} vP(v)} \tag{A-5}$$

where $P(v)$ is the histogram of the length v of the vertical lines.

(5) Trapping time (TT), which indicates the mean length of the vertical lines. It measures the mean time that the system is trapped in one state or changes very slowly. It is given by

$$\mathrm{TT} = \frac{\sum_{v=v_{\min}}^{N} vP(v)}{\sum_{v=v_{\min}}^{N} P(v)} \tag{A-6}$$

(6) Longest vertical line ($V_{\max}$), which is the length of the longest vertical line and is given by

$$V_{\max} = \max(\{v_i; i = 1, \cdots, N_v\}) \tag{A-7}$$

(7) Longest diagonal line ($L_{\max}$), which is the length of the longest diagonal line and is given by

$$L_{\max} = \max(\{l_i; i = 1, \ldots, N_l\}) \tag{A-8}$$

(8) Recurrence times of the 1st and 2nd Poincare recurrence points (T_1 and T_2), which is given by

$$T_1(i) = t_{i+1} - t_i, \quad i = 1, 2, \ldots \tag{A-9}$$

$$T_2(i) = t'_{i+1} - t'_i, \quad i = 1, 2, \ldots \tag{A-10}$$

The calculation details can be found in Webber and Zbilut (1994), Zbilut et al. (2002), Gao et al. (2003) and Marwan et al. (2007). The software for recurrence plot and quantification analysis is available at http://www.recurrence-plot.tk. In this research, the RQA estimators are calculated with a dimension of $m = 1$, a delay of $\tau = 1$, a radius of $\varepsilon = 15$ and distance norm = Euclidean.

Appendix B. Extreme learning machine

B.1 Basic ELM (non-kernel case)

The basic ELM is carried out in the following procedures:Given N distinct samples $(\mathbf{x}_k, \mathbf{t}_k)$, where $\mathbf{x}_k = [x_{k1}, x_{k2}, \ldots, x_{kn}]^{\mathrm{T}}$ is the kth sample with n-dimensional features and $\mathbf{t}_k = [t_{k1}, t_{k2}, \ldots, t_{km}]^{\mathrm{T}}$ represents the actual labels of $\mathbf{x}_k$. Standard single-hidden layer feed-forward neural networks (SLFN) with M hidden neurons can be defined as:

$$\sum_{i=1}^{M} \beta_i g(\mathrm{w}_i \cdot \mathrm{x}_k + b_i) = \mathrm{o}_k, \quad k = 1, \ldots, N, \tag{B-1}$$

where $\mathrm{w}_i = [w_{i1}, w_{i2}, \ldots, w_{in}]^{\mathrm{T}}$ represents the weight vector connecting the ith hidden neuron and the input nodes, $\beta_i = [\beta_{i1}, \beta_{i2}, \ldots, \beta_{im}]^{\mathrm{T}}$ denotes the weight vector connecting the ith hidden neuron and the output nodes, b_i is the threshold of the ith hidden neuron and $\mathrm{o}_k = [o_{k1}, o_{k2}, \ldots, o_{km}]^{\mathrm{T}}$ is the kth output neuron. $g(\bullet)$ denotes the activation function.

If the SLFN with M hidden neurons and activation function $g(\bullet)$ can approach these N training samples with zero error, i.e., $\sum_{k=1}^{N} \|\mathrm{o}_k - \mathrm{t}_k\| = 0$, then β_i, w_i and b_i satisfy the following:

$$\sum_{i=1}^{M} \beta_i g(\mathrm{w}_i \cdot \mathrm{x}_k + b_i) = \mathrm{t}_k, \quad k = 1, \ldots, N, \tag{B-2}$$

The above equations can be compacted as

$$\mathrm{H}\beta = \mathrm{T}, \tag{B-3}$$

where

$$\mathbf{H}(\mathbf{w}_1, \ldots, \mathbf{w}_M, b_1, \ldots, b_M, \mathbf{x}_1, \ldots, \mathbf{x}_N) = \begin{bmatrix} g(\mathbf{w}_1 \cdot \mathbf{x}_1 + b_1) & \ldots & g(\mathbf{w}_M \cdot \mathbf{x}_1 + b_M) \\ \vdots & \ldots & \vdots \\ g(\mathbf{w}_1 \cdot \mathbf{x}_N + b_1) & \ldots & g(\mathbf{w}_M \cdot \mathbf{x}_N + b_M) \end{bmatrix}_{N \times M} \tag{B-4}$$

$$\beta = \begin{bmatrix} \beta_1^T \\ \vdots \\ \beta_M^T \end{bmatrix}_{M \times m} \quad \text{and} \quad \mathbf{T} = \begin{bmatrix} \mathbf{t}_1^T \\ \vdots \\ \mathbf{t}_N^T \end{bmatrix}_{N \times m} \tag{B-5}$$

$\mathbf{H}$ denotes the hidden layer output matrix of the neural network.

Huang et al. (2006) has proved that, given arbitrarily small value $\varepsilon > 0$, if the hidden layer activation function of the SLFN is infinitely differentiable, and the number of hidden neurons is $M \leqslant N$, the input weights and hidden layer biases can be evaluated at random, then the process of training a SLFN becomes to solve a linear system optimization problem as follows:

$$\|\mathrm{H}\hat{\beta} - \mathrm{T}\| = \min_{\beta} \|\mathrm{H}\beta - \mathrm{T}\|, \tag{B-6}$$

where $\hat{\beta} = \mathrm{H}^{\dagger}\mathrm{T}$ is the smallest norm least-squares solution of $\mathrm{H}\beta = \mathrm{T}$, and $\mathrm{H}^{\dagger}$ denotes the Moore–Penrose generalized inverse of H.

The general procedure of ELM is as follows:

Step 1: Assess the input weights $\mathbf{w}_i$ and hidden layer biases b_i randomly;
Step 2: Compute the hidden layer output matrix $\mathbf{H}$;
Step 3: Obtain the output weight $\hat{\beta}$ according to $\hat{\beta} = \mathrm{H}^{\dagger}\mathrm{T}$.

B.2. ELM with kernels

The output of a RBF network with M kernels for an input vector $\mathrm{x} \in \mathrm{R}^d$ is given by

$$f_M(\mathrm{x}) = \sum_{i=1}^{M} \beta_i \phi_i(\mathrm{x}) = \phi(\mu_i, \sigma_i, \mathrm{x}) \tag{B-7}$$

where $\beta_i = [\beta_{i1}, \beta_{i2}, \ldots, \beta_{im}]^{\mathrm{T}}$ denotes the weight vector connecting the ith kernel and the output nodes and $\mu_i = [\mu_{i1}, \mu_{i2}, \ldots, \mu_{in}]^{\mathrm{T}}$ is the ith kernel's center and σ_i is its impact width. ϕ denotes the kernel function.

Similarly to SLFN case, the standard RBFs with M kernels can approximate these N samples with zero error (Huang, 2014) means that $\sum_{k=1}^{N} \|\mathrm{o}_k - \mathrm{t}_k\| = 0$, i.e., there exist β_i, μ_i and σ_i such that

$$\sum_{i=1}^{M} \beta_i \phi(\mu_i, \sigma_i, \mathrm{x}_k) = \mathrm{t}_k, \quad k = 1, \ldots, N. \tag{B-8}$$

The above equations can be compacted as

$$\mathrm{H}\beta = \mathrm{T},$$

where

$$\mathbf{H}(\mu_1, \ldots, \mu_M, \sigma_1, \ldots, \sigma_M, \mathbf{x}_1, \ldots, \mathbf{x}_N) = \begin{bmatrix} \phi(\mu_1, \sigma_1, \mathbf{x}_1) & \ldots & \phi(\mu_M, \sigma_M, \mathbf{x}_1) \\ \vdots & \ldots & \vdots \\ \phi(\mu_1, \sigma_1, \mathbf{x}_N) & \ldots & \phi(\mu_M, \sigma_M, \mathbf{x}_N) \end{bmatrix}_{N \times M} \tag{B-9}$$

$$\beta = \begin{bmatrix} \beta_1^T \\ \vdots \\ \beta_M^T \end{bmatrix}_{M\times m} \quad \text{and } \mathbf{T} = \begin{bmatrix} \mathbf{t}_1^T \\ \vdots \\ \mathbf{t}_N^T \end{bmatrix}_{N\times m}$$

H denotes the hidden layer output matrix of the RBF network.

Thus, similar to SLFNs, the ELM for RBF networks can be summarized as follows:

Step 1: Assign arbitrarily kernel centers μ_i and impact widths σ_i;

Step 2: Calculate the hidden layer output matrix **H**;

Step 3: Compute the output weight $\hat{\beta}$ according to $\hat{\beta} = \mathrm{H}^{\dagger}\mathrm{T}$.

Appendix C. A list of acronyms

A summary of acronyms used in this research is listed in Table C-1.

Table C-1
A summary of acronyms.

Acronym	Full name
ANN	Artificial neural network
ApEn	Approximate entropy
%DET	Determinism
DB	The duration of blink
ECD	Eye closure degree
ECG	Electrocardiography
EEG	Electroencephalography
ELM	Extreme learning machine
ELM_sig	ELM with sigmoid activation function
ELM_RBF	ELM with RBF kernels
EMG	Electromyography
ENTR	The entropy of the frequency distribution of the diagonal line lengths
EOG	Electrooculography
FDR	False detection rate
FES	Fuzzy expert system
Fm	Frontal midline
FPR	False positive rate
FV	Frequency variability
GF	Gravity frequency
HR	Heart rate
IB	The intervals between blinks
IRB	Institutional review board
LAM	Laminarity
L_{max}	Longest diagonal line
NB	The number of blinks
NIR	Near infra-red
PP	Power percentage
RBF	Radial basis function
%REC	Recurrence rate
REM	Rapid eye movement
RenEn	Renyi entropy
ROC	Receiver operating characteristic
ROC–AUC	The area under the ROC curve
RPs	Recurrence plots
RQA	Recurrence quantification analysis
SampEn	Sample entropy
sEMG	Surface electromyography
Sens.	Sensitivity
ShanEn	Shannon entropy
SLFN	Single-hidden layer feed-forward neural networks
SSVEPs	Steady state VEPs
SVM	Support vector machine
TPR	True positive rate
TT	Trapping time
T1	Recurrence times of the 1st Poincare recurrence points
T2	Recurrence times of the 2nd Poincare recurrence points
VEP	Visually evoked potentials
V_{max}	Longest vertical line

References

Al-Angari, H. M., & Sahakian, A. V. (2007). Use of sample entropy approach to study heart rate variability in obstructive sleep apnea syndrome. *IEEE Transactions on Biomedical Engineering, 54*(10), 1900–1904.

Azim, T., Jaffar, M. A., & Mirza, A. M. (2014). Fully automated real time fatigue detection of drivers through fuzzy expert systems. *Applied Soft Computing, 18*, 25–38.

Baker, K., Olson, J., & Morisseau, D. (1994). Work practices, fatigue, and nuclear power plant safety performance. *Human Factors, 36*(2), 244–257.

Boksem, M. A. S., Meijman, T. F., & Lorist, M. M. (2005). Effects of mental fatigue on attention: An ERP study. *Brain Research. Cognitive Brain Research, 25*(1), 107–116.

Borghini, G., Astolfi, L., Vecchiato, G., Mattia, D., & Babiloni, F. (2014). Measuring neurophysiological signals in aircraft pilots and car drivers for the assessment of mental workload, fatigue and drowsiness. *Neuroscience & Biobehavioral Reviews, 44*, 58–75.

Bruce, E. N., Bruce, M. C., & Vennelaganti, S. (2009). Sample entropy tracks changes in EEG power spectrum with sleep state and aging. *Journal of Clinical Neurophysiology, 26*(4), 257–266.

Burioka, N., Miyata, M., Cornélissen, G., Halberg, F., Takeshima, T., Kaplan, D. T., et al. (2005). Approximate entropy in the electroencephalogram during wake and sleep. *Clinical EEG and Neuroscience, 36*(1), 21–24.

Chen, L. L., Sugi, T., Shirakawa, S., Zou, J. Z., & Nakamura, M. (2010). Integrated design and evaluation system for the effect of rest breaks in sustained mental work based on neuro-physiological signals. *International Journal of Control, Automation, and Systems, 8*(4), 862–867.

Chen, L. L., Zhang, J., Zou, J. Z., Zhao, C. J., & Wang, G. S. (2014). A framework on wavelet-based nonlinear features and extreme learning machine for epileptic seizure detection. *Biomedical Signal Processing and Control, 10*, 1–10.

Cornforth, D. J., Tarvainen, M. P., & Jelinek, H. F. (2013). Using Renyi entropy to detect early cardiac autonomic neuropathy. *Conference Proceedings of the IEEE Engineering in Medicine and Biology Society*, 5562–5565.

Cyganek, B., & Gruszczyński, S. (2014). Hybrid computer vision system for drivers' eye recognition and fatigue monitoring. *Neurocomputing, 126*, 78–94.

Dawson, D., Searle, A. K., & Paterson, J. L. (2014). Look before you (s)leep: Evaluating the use of fatigue detection technologies within a fatigue risk management system for the road transport industry. *Sleep Medicine Reviews, 18*(2), 141–152.

De Gennaro, L., Ferrara, M., Ferlazzo, F., & Bertini, M. (2001). The boundary between wakefulness and sleep: Quantitative electroencephalographic changes during the sleep onset period. *Neuroscience, 107*, 1–11.

Dissanayaka, C., Ben-Simon, E., Gruberger, M., Maron-Katz, A., Sharon, H., Hendler, T., & Cvetkovic, D. (2015). Comparison between human awake, meditation and drowsiness EEG activities based on directed transfer function and MVDR coherence methods. *Medical & Biological Engineering & Computing* [Epub ahead of print].

Doughty, M. J. (2002). Further assessment of gender- and blink pattern related differences in the spontaneous eye blink activity in primary gaze in young adult humans. *Optometry and Vision Science, 79*, 439–447.

Eckmann, J. P., Kamphorst, S. O., & Ruelle, D. (1987). Recurrence plots of dynamical systems. *Europhysics Letters, 5*, 973–977.

Folkard, S., & Tucker, P. T. (2003). Shift work, safety and productivity. *Occupational Medicine, 53*, 95–101.

Forsman, P. M., Vila, B. J., Short, R. A., Mott, C. G., & Van Dongen, H. P. (2013). Efficient driver drowsiness detection at moderate levels of drowsiness. *Accident Analysis & Prevention, 50*, 341–350.

Gao, J. B., Cao, Y. H., Gu, L. Y., Harris, J. G., & Principe, J. C. (2003). Detection of weak transitions in signal dynamics using recurrence time statistics. *Physics Letters A, 317*, 64–72.

Garcés Correa, A., Orosco, L., & Laciar, E. (2014). Automatic detection of drowsiness in EEG records based on multimodal analysis. *Medical Engineering & Physics, 36*(2), 244–249.

Hashemi, A., Saba, V., & Resalat, S. N. (2014). Real time driver's drowsiness detection by processing the EEG signals stimulated with external flickering light. *Basic and Clinical Neuroscience, 5*(1), 22–27.

Hu, S. Y., & Zheng, G. T. (2009). Driver drowsiness detection with eyelid related parameters by support vector machine. *Expert Systems With Applications, 36*, 7651–7658.

Huang, G. B. (2014). An insight into extreme learning machines: Random neurons, random features and kernels. *Cognitive Computation, 6*, 376–390.

Huang, G. B., Zhu, Q. Y., & Siew, C. K. (2006). Extreme learning machine: Theory and applications. *Neurocomputing, 70*, 489–501.

Inanaga, K. (1998). Frontal midline theta rhythm and mental activity. *Psychiatry and Clinical Neurosciences, 52*(6), 555–566.

Jagannath, M., & Balasubramanian, V. (2014). Assessment of early onset of driver fatigue using multimodal fatigue measures in a static simulator. *Applied Ergonomics, 45*(4), 1140–1147.

Jiménez-Pinto, J., & Torres-Torriti, M. (2013). Optical flow and driver's kinematics analysis for state of alert sensing. *Sensors-Basel, 13*(4), 4225–4257.

Jo, J., Lee, S. J., Park, K. R., Kim, I. J., & Ki, J. (2014). Detecting driver drowsiness using feature-level fusion and user-specific classification. *Expert Systems with Applications, 41*(4), 1139–1152.

Johnson, R. R., Popovic, D. P., Olmstead, R. E., Stikic, M., Levendowski, D. J., & Berka, C. (2011). Drowsiness/alertness algorithm development and validation using synchronized EEG and cognitive performance to individualize a generalized model. *Biological Psychology, 87*(2), 241–250.

Lal, S. K. L., & Craig, A. (2005). Reproducibility of the spectral components of the electroencephalogram during driver fatigue. *International Journal of Psychophysiology, 55*, 137–143.

Lal, S. K. L., Craig, A., Boord, P., Kirkup, L., & Nguyen, H. (2003). Development of an algorithm for an EEG-based driver fatigue countermeasure. *Journal of Safety Research, 34*, 321–328.

Lee, B. G., Lee, B. L., & Chung, W. Y. (2014). Mobile healthcare for automatic driving sleep-onset detection using wavelet-based EEG and respiration signals. *Sensors (Basel), 14*(10), 17915–17936.

Li, G., & Chung, W. Y. (2014). Estimation of eye closure degree using EEG sensors and its application in driver drowsiness detection. *Sensors (Basel), 14*(9), 17491–17515.

Lin, C. T., Chen, Y. C., Huang, T. Y., Chiu, T. T., Ko, L. W., Liang, S. F., et al. (2008). Development of wireless brain computer interface with embedded multitask scheduling and its application on real-time driver's drowsiness detection and warning. *IEEE Transactions on Biomedical Engineering, 55*(5), 1582–1591.

Liu, J. P., Zhang, C., & Zheng, C. X. (2010). EEG-based estimation of mental fatigue by using KPCA-HMM and complexity parameters. *Biomedical Signal Processing, 5*, 124–130.

Marwan, N., Romano, M. C., Thiel, M., & Kurths, J. (2007). Recurrence plots for the analysis of complex systems. *Physics Reports, 438*, 237–329.

McIntire, L. K., McKinley, R. A., Goodyear, C., & McIntire, J. P. (2014). Detection of vigilance performance using eye blinks. *Applied Ergonomics, 45*(2), 354–362.

Nakamura, M., Chen, Q., Sugi, T., Ikeda, A., & Shibasaki, H. (2005). Technical quality evaluation of EEG recording based on electroencephalographers' knowledge. *Medical Engineering & Physics, 27*, 93–100.

Pincus, S. (1991). Approximate entropy as a measure of system complexity. *Proceedings of the National Academy of Sciences of the United States of America, 88*(6), 297–301.

Renyi A. (1960). On measures of entropy and information. In: *Proc fourth Berkeley symp math stat prob* (Vol. 1, p. 547).

Richman, J. S., & Moorman, J. R. (2000). Physiological time-series analysis using approximate entropy and sample entropy. *American Journal of Physiology: Heart and Circulatory Physiology, 278*(6), 2039–2049.

Shibasaki, H., Nakamura, M., Sugi, T., Nishida, S., Nagamine, T., & Ikeda, A. (2014). Automatic interpretation and writing report of the adult waking electroencephalogram. *Clinical Neurophysiology, 125*(6), 1081–1094.

Singh, R. R., Conjeti, S., & Banerjee, R. (2013). A comparative evaluation of neural network classifiers for stress level analysis of automotive drivers using physiological signals. *Biomedical Signal Processing, 8*(6), 740–754.

Song, I. H., Lee, D. S., & Kim, S. I. (2004). Recurrence quantification analysis of sleep electoencephalogram in sleep apnea syndrome in humans. *Neuroscience Letters, 366*(2), 148–153.

Subasi, A. (2005). Automatic recognition of alertness level from EEG by using neural network and wavelet coefficients. *Expert Systems with Applications, 28*(4), 701–711.

Takahashi, N., Shinomiya, S., Mori, D., & Tachibana, S. (1997). Frontal midline theta rhythm in young healthy adults. *Clinical Neurophysiology, 28*(1), 49–54.

Tucker, P. T., Folkard, S., & Macdonald, I. (2003). Rest breaks and accident risk. *The Lancet, 361*, 680.

Vuckovic, A., Radivojevic, V., Chen, A. C. N., & Popovic, D. (2002). Automatic recognition of alertness and drowsiness from EEG by an artificial neural network. *Medical Engineering & Physics, 24*, 349–360.

Webber, C. L., & Zbilut, J. P. (1994). Dynamical assessment of physiological systems and states using recurrence plot strategies. *Journal of Applied Physiology, 76*, 965–973.

Wu, J. D., & Chen, T. R. (2008). Development of a drowsiness warning system based on the fuzzy logic images analysis. *Expert Systems with Applications, 34*(2), 1556–1561.

Yeo, M. V. M., Li, X. P., Shen, K., & Wilder-Smith, E. P. V. (2009). Can SVM be used for automatic EEG detection of drowsiness during car driving? *Safety Science, 47*, 115–124.

Zbilut, J. P., Thomasson, N., & Webber, C. L. (2002). Recurrence quantification analysis as a tool for nonlinear exploration of nonstationary cardiac signals. *Medical Engineering & Physics, 24*, 53–60.

Zhang, A. H., & Chen, Y. F. (2012). EEG feature extraction and analysis under drowsy state based on energy and sample entropy. In *Proc BMEI* (pp. 501–505).

Zhao, C. L., Zheng, C. X., Zhao, M., Tu, Y. L., & Liu, J. P. (2011). Multivariate autoregressive models and kernel learning algorithms for classifying driving mental fatigue based on electroencephalographic. *Expert Systems with Applications, 38*, 1859–1865.

Zweig, M., & Campbell, G. (1993). Receiver-operating characteristic (ROC) plots: A fundamental evaluation tool in clinical medicine. *Clinical Chemistry, 39*, 561–577.